VIBRATION ALLEVIATION OF A HINGELESS HELICOPTER ROTOR BLADE BY STATE FEEDBACK

E. M. Belo, Mech. Eng., MSc, PhD, MAIAA and
F. D. Marques, Mech. Eng., MSc
Department of Mechanical Engineering,
Engineering School of S. Carlos,
University of São Paulo, Brazil

ABSTRACT

A helicopter blade vibration alleviation strategy is presented in this work. A study is done based on energy methods. The helicopter blade is first modelled by the finite element method being the blade considered as a rotating beam undergoing the coupling motions of flapping, lead-lagging, axial stretching and torsion. The blade is also considered having a pre-twist angle, an offset between mass and elastic axes and being made of isotropic material. After the finite element matrices are obtained, reduced and linearized, a linearized aerodynamic loading is also calculated for hover flight condition and included in the model. Once these dynamic and aerodynamic equations that express the blade vibration motions are obtained, the state-space approach is used to design the control system considering output feedback control strategy. Finally, the system is simulated and the results for open and closed-loop condition are presented. Analysing these results one can observe that they exhibit good response qualities showing that output feedback strategy considered in this work is a good alternative for helicopter vibration attenuation.

INTRODUCTION

The vibration level achieved by a helicopter when flying is a bad characteristic of this kind of aircraft. These vibrations are mainly originated at the helicopter rotor, which is formed by flexible blades excited by oscillatory aerodynamic and inertial forces. The helicopter rotor cannot be totally isolated from the helicopter structure, so these vibrations, originated in the rotor, transfer to the structure and create a hostile environment for most of the helicopter devices, crew and passengers. Trying to decrease and to alleviate these vibrations a great quantity of work has been done in order to obtain a solution to these problems and a considerable progress has already been reached.

To tackle these problems and having in mind vibrations alleviation in helicopters, one has to have a mathematical dynamic model of helicopter blades. To obtain such model various topics should be considered. These topics could be condensed as presented in Figure 1.

Among the ways to reduce vibration problems in helicopters three main ways to tackle the problem can be considered: design of structural and aeroelastic optimised blades; design of passive devices to be added to rotors and blades; and design of active control devices acting on the blades and/or structure. Figure 2 shows this in a succinct form.

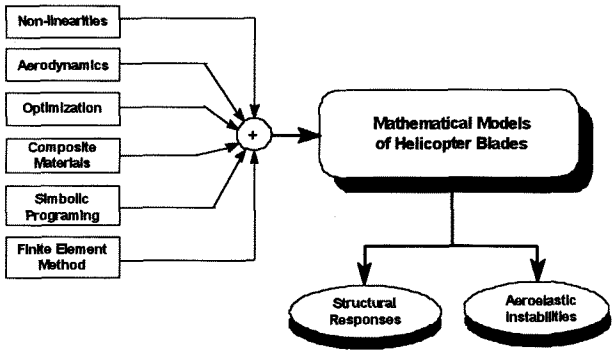

FIGURE 1 - Topics related to the mathematical modelling of helicopter blades

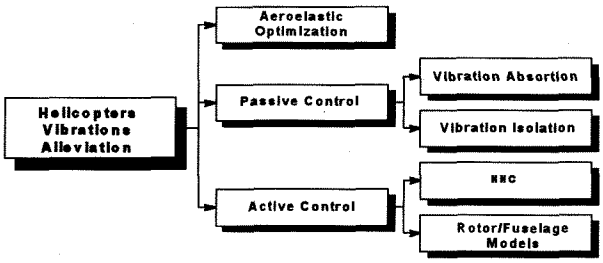

FIGURE 2 - Helicopter vibrations alleviation

The first one tries to eliminate or decrease the helicopter vibratory response through an accurate structural design, e.g., using structural design optimisation techniques involving aerodynamic and structural studies together (Reichert [1]; Loewy [2]). The second one is done by installing devices (dynamic absorbers) in the rotor or fuselage in order to absorb the vibrations, or isolate the vibratory sources (Reichert [1];

Loewy [2]). The third one uses techniques from automatic control systems based on externally powered devices. These devices strategically placed on the vibrating structure produce motions or vibrations opposite to those one wants to eliminate, cancelling them. Some of these strategies are described by Kretz and Larché [3], and Friedmann [4] where their application to helicopters is shown. This last is the one to be considered in this work.

When considering active control techniques two main approaches can be addressed. One is that is referred as classic linear control theory using transfer functions (frequency domain) and the other is the modern one which uses the system represented in state space form (time domain). From these active control systems techniques applied to helicopter vibration suppression, the state space based modern control theory has been intensively used nowadays. Two applications of modern control theory for helicopter vibration reduction have been studied. The first one considers the rotor-fuselage coupling model as showed in Straub [5], Takahashi and Friedmann [6,7]. The second, showed in Jonhson [8], Robinson and Friedmann [9] and Nguyen and Chopra [10,11], considers only the rotor. In this second one, the control is applied by exciting the blade with higher harmonics of the blade rotational speed, called, Higher Harmonic Control - HHC.

However, another kind of state space feedback control approach has been studied for applications in structures. This is the eigenstructure assignment. Using the state-space representation, the control is obtained by assigning a desired eigenstructure to a certain closed-loop system by assessment of the feedback gain matrices. In aeronautics this approach is applied for stability augmentation and autopilots as showed by Stevens and Lewis [12]. For helicopter vibration suppression this approach can be seen in Straub and Warmbrodt [13] who used state feedback.

State feedback is not always an easy task to implement and some times can also be very expensive. So, as an alternative to state feedback, the output feedback eigenstructure assignment technique for helicopter blade vibration control is studied here. For study purposes the blade was considered as a rotating cantilever beam undergoing the three-dimensional bending-torsion coupling motions. The finite element method was used to compose the blade model dynamic equations, which had their order reduced by the partial fractions expansion method. Once having the blade reduced model, the output feedback gain matrix was calculated and applied to the complete (non-reduced) blade model. Then the resulting open and closed-loop systems were simulated and their simulated responses analysed.

MATHEMATICAL MODELLING

The blade studied here is modelled as a rotating cantilever beam with length R, undergoing the coupling motions of flapping, lead-lagging, axial stretching and torsion as in Houlbolt & Brooks [14], Hodges & Dowell [15], and Marques [16]. A pre-twist angle θ_t is adopted in the model, considered null in the blade root and varying linearly along the span. It is also supposed that elastic and mass axes are non-coincidents.

In order to develop the model equations, different co-ordinate systems have to be considered. The main co-ordinate systems of the blade model are shown in Figures 3 and 4. The first one shows the main co-ordinate system x, y and z, that is fixed in the blade root with its origin in the intersection of blade root cross-section and elastic axis. When the blade is not deformed the x axis is exactly coincident with the elastic axis. Figure 3 also shows the deformed blade and elastic displacement u, v and w, in the x, y and z directions, respectively. Figure 4 shows an arbitrary blade cross-section and its local co-ordinate system η and ζ. The torsional deflection ϕ, due to the blade deformation can also be seen.

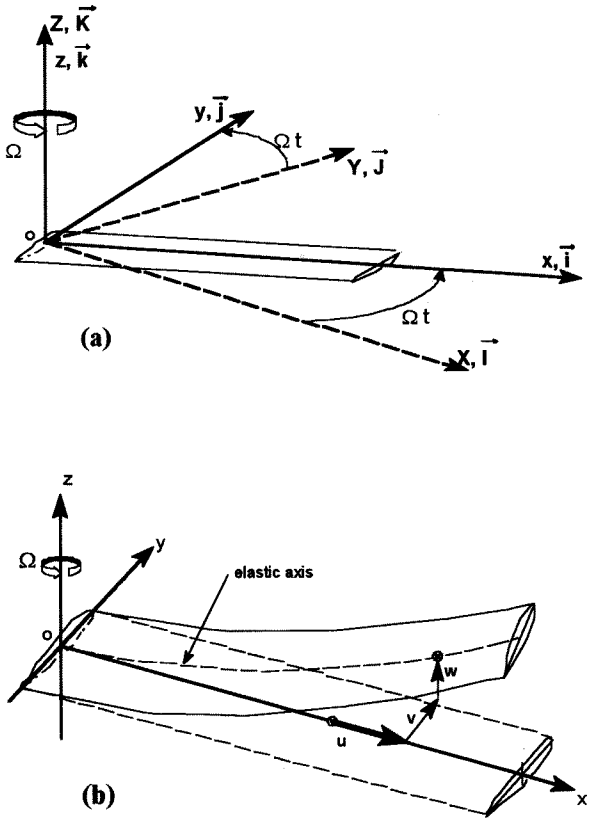

FIGURE 3 - Blade co-ordinate systems and elastic displacements **(a)** before and **(b)** after deflection

To obtain the dynamic equations the formulation for strain and kinetic energy are used as well as steady aerodynamic approach with some simplifications.

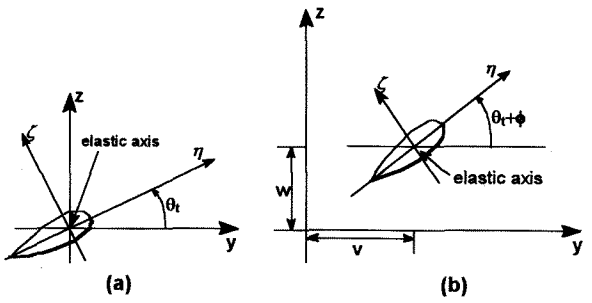

FIGURE 4 - Cross-sectional co-ordinate system (a) before and (b) after deflection.

Strain energy of a rotating beam

Supposing a rotating beam undergoing axial stress, shear in the lead-lagging plane and in the flapping plane, the strain energy is given by:

$$V = \frac{1}{2}\int_0^R \Big\{ EAu'^2 + EI_z\left(v''\cos\theta_t + w''sin\theta_t\right)^2 + \\ +EI_y\left(-v''sin\theta_t + w''\cos\theta_t\right)^2 + \\ +GJ\,\phi'^2 + F_c v'^2 + F_c w'^2 \Big\}\, dx \qquad (1)$$

where EA, EI_y, EI_z and GJ are the axial, lead-lagging, flapping and torsional stiffness, respectively; u', v', w', ϕ' the first order partial derivatives of u, v, w and ϕ with relation to x and v'', w'' the second order ones. The term F_c is the centrifugal effect and is a function of the mass m and the blade rotational speed Ω:

$$F_c = \int_x^R \Omega^2\, m\, x\, dx \qquad (2)$$

Kinetic energy of a rotating beam

To obtain the kinetic energy expression, the approach presented by Magari et al [17] is used here and is:

$$T = \frac{1}{2}\int_0^R \left\{ \iint_A (\rho\, d\eta\, d\zeta)\left(\frac{d\vec{r}}{dt}\bullet\frac{d\vec{r}}{dt}\right)\right\} dx \qquad (3)$$

where ρ is the density and the other variables are according to the sketch of Figure 5 and 6.

The velocity of an arbitrary point in the blade cross-sections is given by:

$$\frac{d\vec{r}}{dt} = \vec{\omega}\times\vec{r} + \dot{\vec{r}} \qquad (4)$$

where:

$$\vec{\omega} = \Omega\vec{k}\ ; \quad \vec{r} = x_1\vec{i} + y_1\vec{j} + z_1\vec{k} \qquad (5)$$

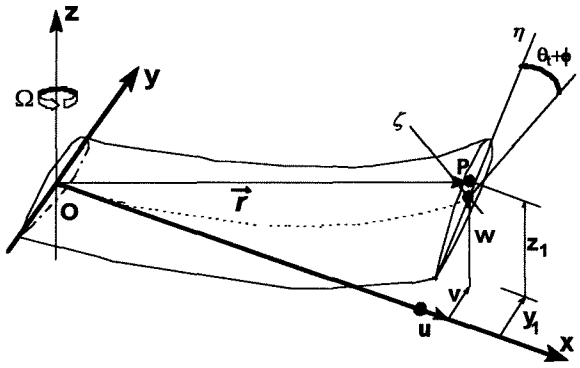

FIGURE 5 - Position of an arbitrary point P of the beam in a cross-section

The co-ordinates (x_1, y_1, z_1) of an arbitrary point in the deformed blade cross-section are the same as shown in references [14] and [16].

The kinetic energy is obtained by substituting equation (4) into equation (3) and calculating the double integrals for the blade cross-section areas. Since this expression is too long it will not be presented in this paper.

The Aerodynamic loading on a helicopter blade

The steady aerodynamic approach was adopted to yield the expressions of lift (L), drag (D) and aerodynamic moment (M) in the hover condition. Some simplifications were adopted. The first one is neglecting the induced velocity, which yields a free air flow velocity parallel to the y axis. The small displacement consideration results in the assumption that the blade cross-section remains parallel to the yz plane. There is no coincidence between mass and elastic axes, but the aerodynamic centre is taken at the same point of the elastic axis and cross-section intersection. The profile NACA 0015 was assumed, therefore, the aerodynamic and the pressure centre of the blade cross-section are the same.

The helicopter blade is divided in elements of length dx, as in Figure 6, and then the corresponding element loads dL (lift), dD (drag), and dM (moment) were calculated.

Considering that the blade elastic displacements in the free air flow and supposing an operational region of the blade angle of attack as shown in Figure 7, a matricial expression representing the aerodynamic loading, results as follows in equation (6).

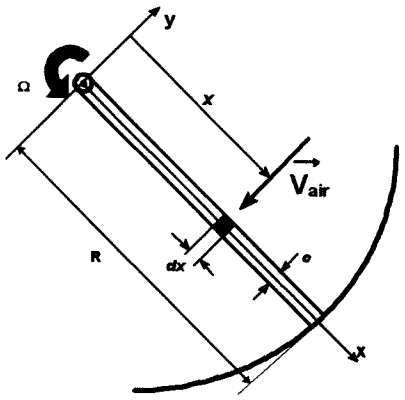

FIGURE 6 - Top view of a helicopter blade showing the positioning of an element *dx*

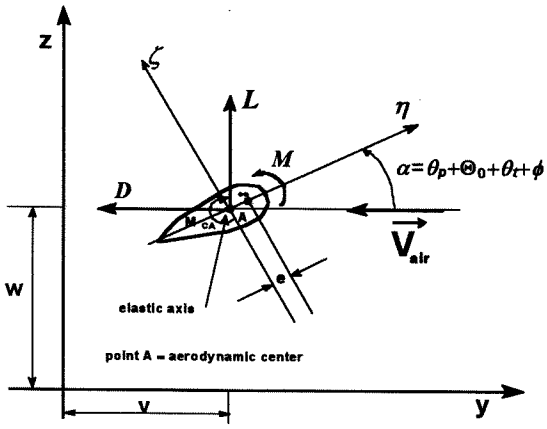

FIGURE 7 - Schematic representation of the helicopter blade cross section under deflection

$$\begin{bmatrix} D \\ L \\ M \end{bmatrix} = \frac{\rho_{air}\, c}{2} \begin{bmatrix} b \\ a \\ ae \end{bmatrix} \int_x^R \left(\theta_P + \Theta_0 + \theta_t + \phi\right) \left\{ \left[\dot{u} - \Omega v\right]^2 + \left[\dot{v} + \Omega\left(x+u\right)\right]^2 + \dot{w}^2 \right\} dx \tag{6}$$

where a and b are the proportionality factors between lift and drag coefficients due to angle of attack, respectively (as $C_L = a \times \alpha$ and $C_D = b \times \alpha$); e is the offset between elastic and mass axis; ρ_{air} is the air mass density; c is the blade cross-section chord; θ_P is the commanded pitch angle; Θ_0 is the nominal value of pitch angle in the operational region (10° in this work).

Finite element method applied to the beam

The finite element method is used to discretize the beam and is done in terms of beam elements, with two nodes, one at each end, as shown in Figure 8.

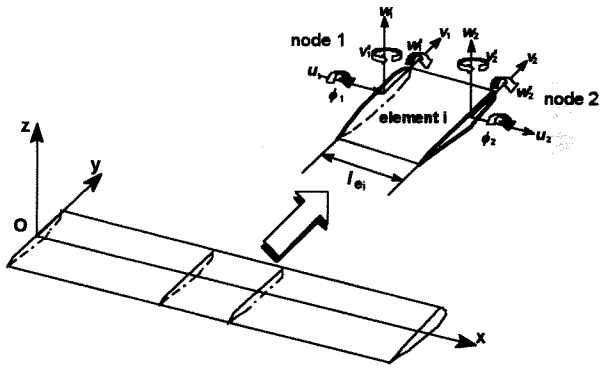

FIGURE 8 - Dicretization of the helicopter blade in finite elements

Each node has six degrees of freedom: displacements in the x, y and z directions, rotation in the xy, xz planes and in the cross-section plane. The nodal displacements (generalised co-ordinates) form the **q** vector and are related with blade displacements through the following equations:

$$\begin{aligned} u &= H_1(x)u_1 + H_2(x)u_2 \\ v &= H_3(x)v_1 + H_4(x)v_1' + H_5(x)v_2 + H_6(x)v_2' \\ w &= H_3(x)w_1 + H_4(x)w_1' + H_5(x)w_2 + H_6(x)w_2' \\ \phi &= H_1(x)\phi_1 + H_2(x)\phi_2 \end{aligned} \tag{7}$$

where $H_1(x)$ through $H_6(x)$ are the shape functions given by third degree Hermite polynomials, which are the same as in Magari et al [17] and Sivaneri & Chopra [18].

Now, the matrices $\mathbf{M_e}$, $\mathbf{G_e}$ and $\mathbf{K_e}$, of each finite element can be obtained. Each coefficient m_{ij}, g_{ij} and k_{ij}, for $i,j = 1,2,...n$, is obtained by substituting equation (7) in the expressions of the strain and kinetic energy. However, these coefficients are not linear in **q**, the linearization occurs adopting the hypothesis of small motions about the equilibrium point (Meirovitch [19]), what yields the expressions of the coefficients as follows:

$$\begin{aligned} m_{ij} &= \left.\frac{\partial^2 T}{\partial \dot{q}_i\, \partial \dot{q}_j}\right|_{q=0} \\ g_{ij} &= \left.\frac{\partial^2 T}{\partial \dot{q}_j\, \partial q_i}\right|_{q=0} - \left.\frac{\partial^2 T}{\partial \dot{q}_i\, \partial q_j}\right|_{q=0} \\ k_{ij} &= \left.\frac{\partial^2 V}{\partial q_i\, \partial q_j}\right|_{q=0} - \left.\frac{\partial^2 T}{\partial q_i\, \partial q_j}\right|_{q=0} \end{aligned} \tag{8}$$

The same procedure is done in order to obtain the loading vector **Q**. By substituting equation (7) in equation (6), non-linear loading expressions are obtained and

linearized next. This loading vector **Q** is composed by two parts. A first one depends only of system inputs and a second one depends only of system generalised co-ordinates.

The system matrices are formed [19] by superposing each $\mathbf{M}_e$, $\mathbf{G}_e$ and $\mathbf{K}_e$, respectively, and considering the system constraints.

The damping effect was put into the model by using the Rayleigh approach described in Clough and Penzien [20]. The damping matrix $\mathbf{C}_a$ is given by $\mathbf{C}_a = a_0 \mathbf{M} + a_1 \mathbf{K}$, where a_0 and a_1 are arbitrary proportionality factors. In this work $a_0 = 3.4843$ and $a_1 = 0.0006$, what yields a damping factor of $\xi = 0.05$.

The mathematical model obtained results in the following matricial equation of motion:

$$\mathbf{M}\ddot{\mathbf{q}} + (\mathbf{G} + \mathbf{C}_a)\dot{\mathbf{q}} + \mathbf{K}\mathbf{q} = \mathbf{Q}(\theta_P, \mathbf{q}, \dot{\mathbf{q}}) \qquad (9)$$

State-space representation

Thinking about application of control techniques, it is convenient to transform the equation (9) into state-space representation.

Taking the state vector $x(t) = [\, \mathbf{q}^T \;\; (d\mathbf{q}/dt)^T \,]^T$, and pre-multiplying the equation (9) by $\mathbf{M}^{-1}$, it follows that [19]:

$$\dot{x}(t) = A\,x(t) + B\,\mathbf{Q} \qquad (10)$$

where A is the state matrix and B is the input matrix.

The loading vector **Q**, when represented in state-space form can be written as $\mathbf{Q}_1\, x(t) + \mathbf{Q}_2\, u(t)$, where $u(t)$ is the control input vector.

Taking each part of the loading vector and substituting them in equation (10), it results:

$$\begin{aligned} \dot{x}(t) &= A_1\, x(t) + B_1\, u(t) \\ y(t) &= C\, x(t) \end{aligned} \qquad (11)$$

where $A_1 = A + B\,\mathbf{Q}_1$, $B_1 = B\,\mathbf{Q}_2$, $y(t)$ is the output vector and C is the output matrix.

This can be represented in terms of block diagram as shown in Figure 8.

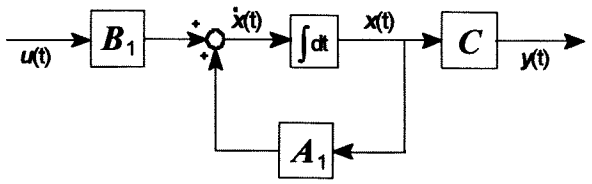

FIGURE 8 - Block diagram corresponding to the complete dynamic equations of the helicopter rotor blade

BEAM MODEL REDUCTION

The high order of the original blade model makes it difficult to work with and some high frequencies that appear do not have great importance since the energy involved is small. So in order to have a better perception of what is happening, it is necessary to use a model reduction procedure. The technique adopted here is the same as that described by [12]. It uses the original system represented in the form of a transfer function matrix written as a partial fraction expansion:

$$\mathbf{H}(s) = \sum_{j=1}^{2n} \frac{\mathbf{C}\,\mathbf{h}_{1j}\,\mathbf{f}_{1j}^T\,\mathbf{B}_1}{s - \lambda_{1j}} \qquad (12)$$

where the $\mathbf{h}_{1j}$, $\mathbf{f}_{1j}$, are the right and left eigenvectors of matrix $\mathbf{A}_1$ respectively, and the λ_{1j} are the corresponding eigenvalues.

Selecting then a set of r eigenvalues, which will remain in the equation (12), and applying the appropriate transformation [12], the result is the reduced orthonormal eigenvectors **U** and **V**, which are applied in the equation (11) by $x_r(t) = \mathbf{V}\, x(t)$. Then, the reduced order model obtained is:

$$\begin{aligned} \dot{x}_r(t) &= A_r\, x_r(t) + B_r\, u(t) \\ y\,(t) &= C_r\, \mathbf{x}_r(t) + D_r\, u(t) \end{aligned} \qquad (13)$$

where, $\mathbf{A}_r = \mathbf{V}\,A_1\,\mathbf{U}$, $B_r = \mathbf{V}\,B_1$, $C_r = C\,\mathbf{U}$ and D_r is given by those eigenvalues of A_1 that were neglected from the system. This model reduction equation above can be represented by the following Figure 9.

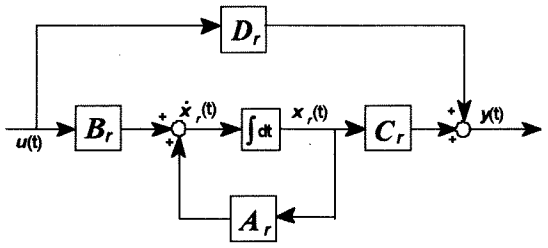

FIGURE 9 - Block diagram corresponding to the reduced dynamic equations of the helicopter rotor blade

CONTROL SYSTEM DESIGN

The control strategy that was idealised was that for the case of a typical blade pitch control linkage. At a first moment an actuator that responds very fast is placed at the pitch control rod and its action on the blade pitch depends on the measure of displacements or velocities got

from some sensors placed along key points on the blade span. Therefore, the idea is to alleviate vibrations on the blade through changes of its pitch angle. A schematic view of the positioning of actuators and sensors on the helicopter blade can be seen in Figure 10.

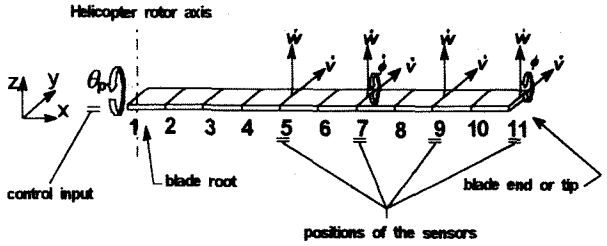

FIGURE 10 - Sketch of a helicopter blade showing the positioning of actuator and sensors for vibration alleviation

The eigenstructure assignment technique by output feedback is applied to yield a gain matrix $\boldsymbol{R}$, that leads to the control system described above.

Due to the size of the original system given by the equation (11), the control law design will be developed by using the reduced model equations.

For output feedback and for the case of a regulator, the control inputs are:

$$\boldsymbol{u}(t) = -\boldsymbol{R}\, \boldsymbol{y}(t) \tag{14}$$

Substituting the equation (14) in the equation (13) and working algebraically, one reaches the following closed-loop equation:

$$\dot{\boldsymbol{x}}_r(t) = \left[\boldsymbol{A}_r - \boldsymbol{B}_r \left(\boldsymbol{I} + \boldsymbol{R}\,\boldsymbol{D}_r\right)^{-1} \boldsymbol{R}\,\boldsymbol{C}_r\right] \boldsymbol{x}_r(t) \tag{15}$$

For assessment of the matrix $\boldsymbol{R}$, a set of eigenvalues and eigenvectors must be assigned in order to yield the desired time response characteristics of the closed-loop system.

Therefore, for each eigenvalue and its respective eigenvector, the null space of $[\,(\boldsymbol{A}_r - \lambda_j^d \boldsymbol{I})\ \boldsymbol{B}_r\,]$ (for j=1,2,..,n) must be taken, which gives another vector, where after its decomposition, results in:

$$\begin{aligned} &\left[\mathbf{q}_1^d \quad \mathbf{q}_2^d \quad \cdots \quad \mathbf{q}_p^d\right] = \\ &= -\left(\boldsymbol{I} + \boldsymbol{R}\,\boldsymbol{D}_r\right)^{-1} \boldsymbol{R}\,\boldsymbol{C}_r \left[\mathbf{v}_1^d \quad \mathbf{v}_2^d \quad \cdots \quad \mathbf{v}_p^d\right] \end{aligned} \tag{16}$$

where p is the number of assigned eigenvalues and $\mathbf{v}^d$ and $\mathbf{q}^d$ result from the null space of $[\,(\boldsymbol{A}_r - \lambda_j^d \boldsymbol{I})\ \boldsymbol{B}_r\,]$.

From equation (16), one obtains:

$$\begin{aligned} \boldsymbol{R} = -\left[\mathbf{q}_1^d \quad \mathbf{q}_2^d \quad \cdots \quad \mathbf{q}_p^d\right] \Big[\boldsymbol{D}_r \left[\mathbf{q}_1^d \quad \mathbf{q}_2^d \quad \cdots \quad \mathbf{q}_p^d\right] + \\ + \boldsymbol{C}_r \left[\mathbf{v}_1^d \quad \mathbf{v}_2^d \quad \cdots \quad \mathbf{v}_p^d\right]\Big]^+ \end{aligned} \tag{17}$$

where $[\ ]^+$ represents the Moore-Penrose pseudo-inverse, since the number of assigned eigenvalues may be different of the number of measured outputs. The closed loop resulting system can be represented in terms of block diagram as it is shown in Figure 11.

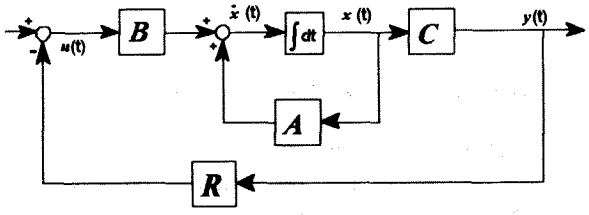

FIGURE 11 - Block diagram of the closed loop control system of the helicopter rotor blade

RESULTS

The softwares **Mathematica** and **MATLAB** were used to obtain the blade model and to assess the gain matrix $\boldsymbol{R}$ for the controller. The numerical values are the same as in [16]. Ten finite elements for the blade model were used giving a free-free system with 66 degrees of freedom (DOFs) which correspond to 11 nodes. With some constraints, that the blade can be considered subjected they turn 51 DOFs. These constraints are: there are no DOFs in the axial (longitudinal) direction and on node 1 only the torsional motion in the x direction of the blade is possible To reduce this model is a desired alternative in order to avoid a greater computational effort. The reduced model was applied considering the first 5 natural frequencies of the blade model with the effect of aerodynamic loading (matrix $\boldsymbol{A}_1$). It leads to a reduced model with dimension equal to 10. The choice of the frequencies results from the fact that the vibratory behaviour of the blade is more damaging at low frequencies.

It is necessary to verify whether the reduced model obtained can represent efficiently the original one. This verification can be done by several ways. One of them is to confront the output from each one for the same input. Figure 12 shows an output of the original model plotted against the corresponding one of the reduced model. The plot tends to stay near a line with 45° of slope. This shows the agreement between the two models. The simulation of the original and reduced models was done for a step input with all state variables considered as output measures, which were compared one to one, showing agreement.

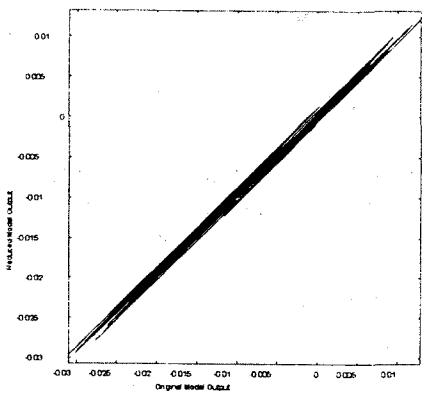

FIGURE 12 - Reduced and original models comparison

The first step to apply the control strategy is to choose where to put the sensors and the control inputs. The characteristics of the closed-loop system depend directly on this choice. As described previously the control input was chosen to be the blade pitch angle in the root. The sensors were placed on the nodes of the blade finite element model, measuring the flapping and lead-lagging velocities on nodes 5, 7, 9 an 11 (blade tip), the torsional gyro ratio on node 7 and the torsional gyro on node 11.

Some criteria were adopted for placing the sensors and for choosing the measured variables. The choice of those nodes was based on the fact that at the blade tip, the displacements as well as the velocities are more significant quantities. An increased blade damping is desired to the resulting closed-loop system, and this is achieved feeding back velocities. The measuring of torsional variables such as, gyro ratio and gyro on blade tip, can warrant a quick stabilisation on torsional variables, what is important in order to avoid problems such as blade stall or even flutter.

Another step to be taken toward the closed-loop system assessment is to assign the eigenstructure, namely, eigenvalues and eigenvectors. The desired time response, frequencies and damping factors for the closed-loop system were the main factors for the eigenvalues choice. Table 1 shows the assigned and the achieved eigenvalues for the closed-loop system. Since the eigenstructure assignment technique was applied using the blade reduced model, only 10 eigenvalues are presented in Table 1. The achieved ones are those from the non-reduced blade model. Only the eigenvalues related to the assigned ones in the reduced model are shown. The other eigenvalues, which are omitted form Table 1, were too little affected by feedback. For the eigenvectors, since there is only one control input, it is impossible to modify them. Next, the time simulations of the blade when in closed loop and open-loop configuration are presented in Figures 13 to 18.

An impulse input of 1.5° of blade pitch angle at the root, was considered with the objective of observing the blade transient response. The variables of simulation that were measured are those at the blade tip.

ASSIGNED EINGENVALUES	ACHIEVED EIGENVALUES
-3.4047±50.798 *i*	-3.4061±50.790 *i*
-12±120 *i*	-12.001±119.94 *i*
-173.62	-161.10
-200	-15.381±205.37 *i*
-15.323±205.48 *i*	-233.08
-31.024±311.71 *i*	-30.915±311.75 *i*

TABLE 1 - Assigned and achieved eigenvalues

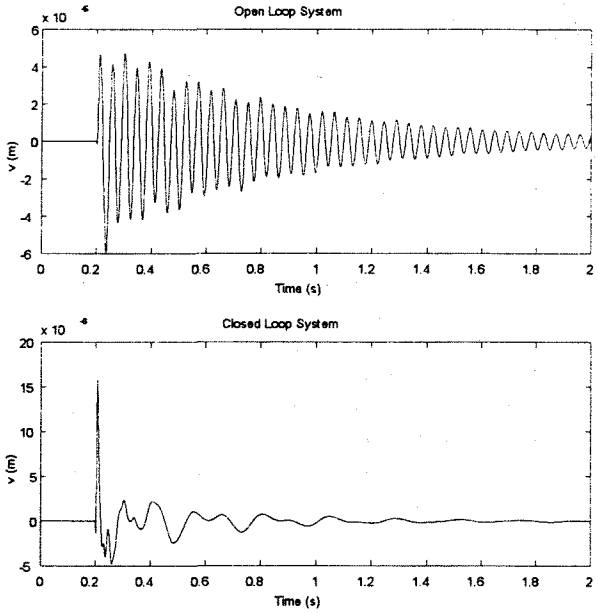

FIGURE 13 - Blade tip displacement: *v*

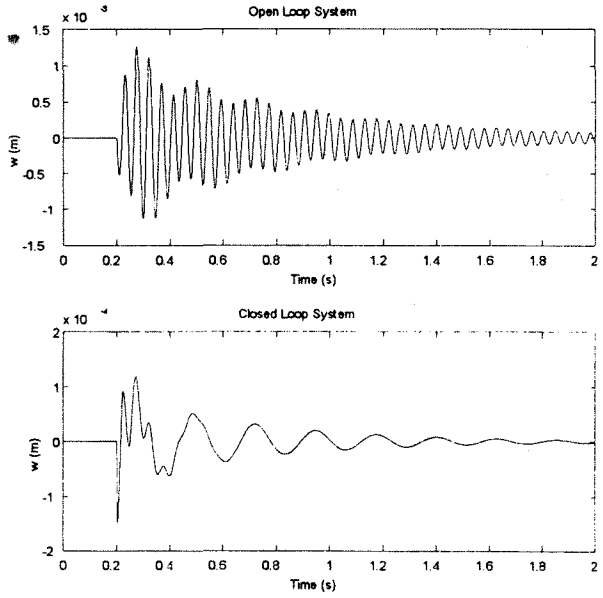

FIGURE 14 - Blade tip displacement: *w*

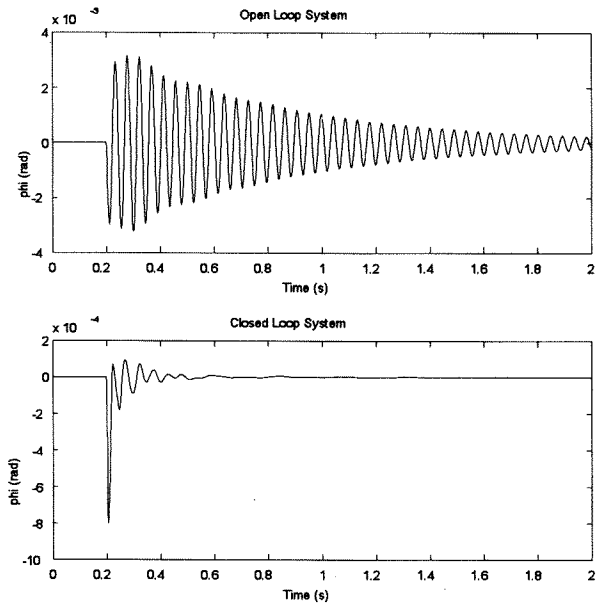

FIGURE 15 - Blade tip angular displacement: ϕ

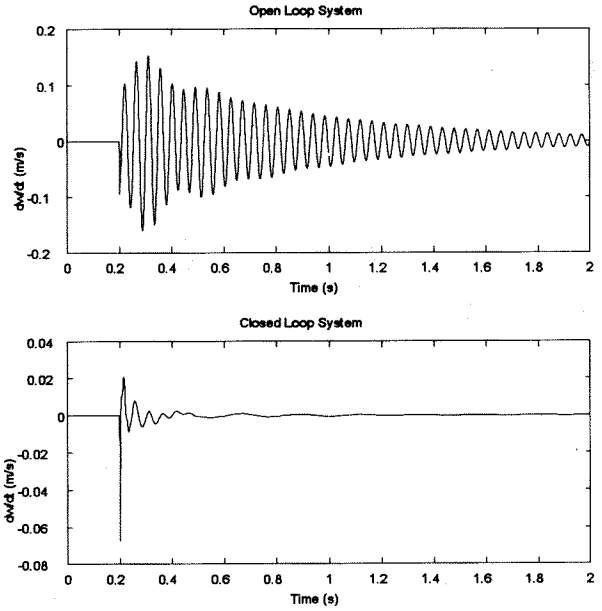

FIGURE 17 - Blade tip velocity: dw/dt

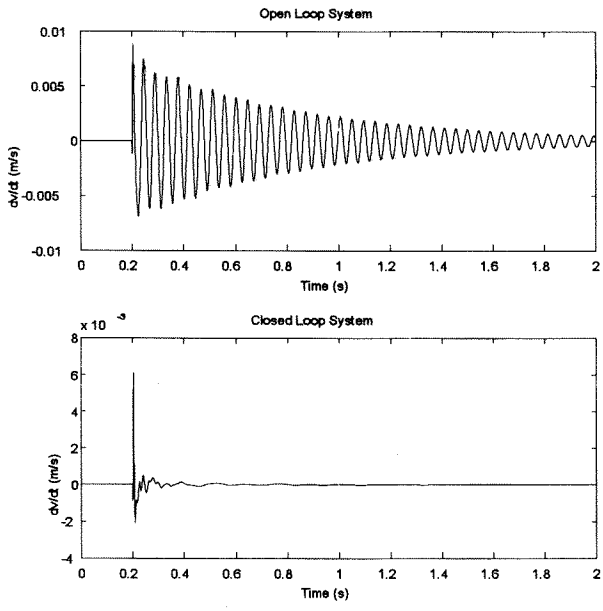

FIGURE 16 - Blade tip velocity: dv/dt

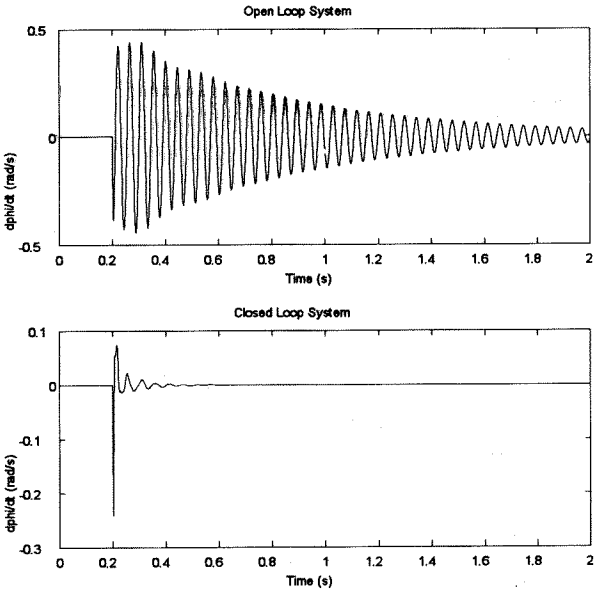

FIGURE 18 - Blade tip angular velocity: dϕ/dt

In the simulated cases, the controller showed efficiency with respect to blade vibration attenuation. However, for some variables, the time response did not present an adequate damping, but shows a good decrease on their response values.

Due to the size of the blade model, the number of sensors used for feedback and the number of control inputs, the range of assignable eigenvalues becomes restricted and some modes can not be modified as it would be desirable.

CONCLUSIONS

A study about the vibration control on a helicopter blade using the eigenstructure assignment by output feedback was presented. Through the results presented it was verified that the reduced order method adopted led to a suitable blade reduced model. As a form of reducing the vibration on a helicopter blade, the eigenstructure assignment by output feedback shows to be efficient, and a promising alternative for further studies. It was also observed through simulation that for some variables the response did not achieve the desired characteristics, what is due to the restricted range of assignable eigenvalues. In spite of this, one can understand from this work that the application of eigenstructure assignment by output feedback for vibration control in a helicopter blade is important and must be studied more deeply.

REFERENCES

1. Reichert, G., 1981, Vertica, 5, 1-20

2. Loewy, R.G., 1984, J.Am. Helic. Soc., 29, 4-30

3. Kretz,M. and Larché,M., 1980, Vertica,4, 13-22

4. Friedmann, P.P.,1990,Vertica, 14, 101-121

5. Straub, F.K., 1987, Vertica, 11, 425-435

6. Takahashi,M.D. and Friedmann,P.P., 1988, Proc. AIAA/ASME/ASCE/AHS Strut, Strut Dyn & Mat Conf, 1521-1532

7. Takahashi, M.D. and Friedmann, P.P., 1991, J. Guid, Control & Dyn, 14, 1294-1300

8. Johnson, W., 1982, NASA TP-1996

9. Robinson, L.H. and Friedmann, P.P., 1989, Proc. AIAA/ASME/ASCE/AHS Strut, Strut Dyn & Mat Conf, 1349-1406

10. Nguyen,K. and Chopra,I., 1990, J.Am. Helic. Soc., 35, 78-89

11. Nguyen, K. and Chopra, I., 1990, Vertica, 14, 545-556

12. Stevens, B.L. and Lewis, F.L., 1992, "Aircraft control and simulation", J. Wiley & Sons, USA

13. Straub, F.K. and Warmbrodt, W., 1985, J.Am. Helic. Soc., 30, 13-22

14. Houlbolt, J.C. and Brooks, G.W., 1958, NACA Report 1346.

15. Hodges, D.H. and Dowell, E.H., 1974, NASA TN D-7818.

16. Marques, F.D., 1993, M.Sc. thesis, University of Sao Paulo, Brasil

17. Magari, P.J., Shultz, L.A. and Murthy, V.R., 1988, Comp. & Struct., 29, 763-776

18. Sivaneri, N.T. and Chopra, I., 1982, AIAA J., 20, 716-723

19. Meirovitch, L., 1990, "Dynamics and control of structures", John Wiley & Sons, New York, USA

20. Clough,R.W. and Penzien,J., 1975, "Dynamics of structures", McGraw-Hill, New York, USA